ELSEVIER

J. Non-Newtonian Fluid Mech. 138 (2006) 7–21

Journal of Non-Newtonian Fluid Mechanics

www.elsevier.com/locate/jnnfm

Fully-developed heat transfer in annuli for viscoelastic fluids with viscous dissipation

F.T. Pinho [a,b,*], P.M. Coelho [c]

[a] *Centro de Estudos de Fenómenos de Transporte, Faculdade de Engenharia, Universidade do Porto, rua Dr. Roberto Frias s/n, 4200-465 Porto, Portugal*

[b] *Universidade do Minho, Largo do Paço, 4704-553 Braga, Portugal*

[c] *Centro de Estudos de Fenómenos de Transporte, DEMEGI, Faculdade de Engenharia, Universidade do Porto, rua Dr. Roberto Frias s/n, 4200-465 Porto, Portugal*

Received 7 December 2005; received in revised form 4 April 2006; accepted 4 April 2006

Abstract

Analytical solutions are obtained for heat transfer in concentric annular flows of viscoelastic fluids modeled by the simplified Phan-Thien–Tanner constitutive equation. Solutions for thermal and dynamic fully developed flow are presented for both imposed constant wall heat fluxes and imposed constant wall temperatures, always taking into account viscous dissipation.

Equations are presented for the normalized temperature profile, the bulk temperature, the inner and outer wall temperatures and, through their definitions for the inner and outer Nusselt numbers as a function of all relevant non-dimensional parameters. Some special results are discussed in detail. Given the complexity of the derived equations, for ease of use compact exact expressions are presented for the Nusselt numbers and programmes to calculate all quantities are made accessible on the internet. Generally speaking, fluid elasticity is found to increase the heat transfer for imposed heating at the wall, especially in combination with internal heat generation by viscous dissipation, whereas for imposed wall temperatures it reduces heat transfer when viscous dissipation is weak.

Keywords: Phan-Thien–Tanner fluid; Annular flow; Internal viscous dissipation; Imposed wall temperatures; Imposed wall heat fluxes

1. Introduction

The concentric annulus is commonly found in heat exchangers and has consequently been the subject of countless research [1,2]. The vast majority of research work has concentrated on the behavior of Newtonian fluids, and much less is known for non-Newtonian fluids, in particular those obeying differential constitutive equations. For these fluids, such as polymer melts, usually possessing viscoelastic properties and high viscosity, heat transfer in the laminar annular flow of viscoelastic fluids is quite important in tube extrusion [3]. From an industrial point of view, the analytical solutions presented here provide the simplest and most efficient way to perform parametric investigations of the effects of independent variables on output quantities. In addition, these solutions serve as test cases for validating numerical solutions and have a pedagogical interest.

The objective of this work is to present analytical heat transfer solutions for the annular flow of viscoelastic fluids of high viscosity, i.e. including effects of viscous dissipation. The simplified form of the Phan-Thien–Tanner constitutive equation (PTT) [4,5] is considered, which includes the Upper Convected Maxwell (UCM) [6] model as a special case.

A consequence of the large viscosity, typical of many viscoelastic fluids, is the fast dynamic flow development. Although the thermal behavior develops slower, the case of simultaneous fully-developed dynamic and thermal flow can be important and is addressed for two different sets of thermal wall boundary conditions: imposed heat fluxes and imposed wall temperatures. In both cases the imposed conditions are uniform at each wall, i.e. they can take identical or different values at the inner and outer walls. The combined situation with imposed heat flux at one wall and imposed wall temperature at the other wall is not addressed here. The general solutions remain valid even when the Brinkman number is set to zero (negligible viscous dissipation), except for identical wall temperatures which requires a completely different approach.

* Corresponding author.
E-mail addresses: fpinho@fe.up.pt (F.T. Pinho), pmc@fe.up.pt (P.M. Coelho).

0377-0257/$ – see front matter © 2006 Elsevier B.V. All rights reserved.
doi:10.1016/j.jnnfm.2006.04.002

Nomenclature

Br	Brinkman number, Eq. (15) for imposed wall heat flux and Eqs. (33) and (34) for imposed wall temperature
c_p	specific heat
D_H	hydraulic diameter, $D_H \equiv 2\delta$
h	heat transfer coefficient
k	thermal conductivity
Nu	Nusselt number, $Nu = 2\delta h/k$
$p_{,x}$	axial pressure gradient
Pr	Prandtl number, $Pr = \eta c_p/k$
$\dot{q}$	heat flux
r	radial coordinate
Re	Reynolds number, $Re = \rho U 2\delta/\eta$
R_i	inner radius of concentric annulus
R_o	outer radius of concentric annulus
T	fluid temperature
$\bar{T}$	mass-averaged temperature
T^+	normalised temperature for the uniform wall heat flux case, Eq. (13a)
T'	normalised temperature for the uniform wall heat flux case, Eq. (13b)
T^*	normalised temperature for the uniform wall temperature case, Eqs. (30a) and (30b)
T_g	glass transition temperature
u	axial velocity
u^+	normalised axial velocity, $u^+ = u/U$
U	bulk velocity
U_c	characteristic velocity, $U_c = -p_{,x}\delta^2/(8\eta)$
x	axial coordinate
x'	normalized axial coordinate, $x' = 2x/(\delta RePr)$
X	ratio of characteristic and bulk velocities
y^+	radius normalised by the inner radius, $y^+ = r/R_i = r/(\delta Y)$
y_*^+	non-dimensional zero shear stress radius
Y	geometric parameter, $Y = \kappa/(1-\kappa)$
We	Weissenberg number, $We = \lambda U/\delta$

Greek letters

α	parameter in energy Eqs. (10a) and (10b)
δ	annular gap ($\delta \equiv R_o - R_i$)
ε	extensional parameter of the PTT model
λ	relaxation time of the PTT model
Φ	ratio of outer and inner wall heat fluxes, $\Phi \equiv \dot{q}_o/\dot{q}_i$
η	coefficient of viscosity of PTT model
κ	radius ratio ($\kappa = R_i/R_o$)
τ_{rx}	shear stress
Ω	geometric parameter,

Subscripts

i	refers to inner wall
in	refers to inlet
o	refers to outer wall
w	refers to any wall

Fluid properties are considered independent of temperature and consequently the fluid dynamic problem is decoupled from the thermal problem. Variation of fluid properties with temperature can account for important differences, but leads to a more complex solution requiring numerical treatment which is left for future investigation. The thermal developing flow case for fully developed dynamics, the so-called Graetz problem, is also not analysed here.

The solution of the fully developed isothermal laminar annular flow for Newtonian fluids was obtained in the XIXth century following the seminal work of Boussinesq in 1868 [1,7]. For non-Newtonian fluids Fredrikson and Bird [8] obtained the solution for a power law fluid and Hanks [9] derived the solution for Herschel-Bulkley materials, for both sets of boundary conditions. For the same form of the PTT constitutive model, Pinho and Oliveira [10] derived the annular isothermal flow solution, but the more general and slightly different expression of Cruz and Pinho [11] is preferred as starting point of the present work. An extensive bibliography on annular flows of non-Newtonian fluids can be found in Escudier et al. [12].

In the absence of viscous dissipation and provided the fluid dynamic and thermal problems are decoupled, the energy equation for purely viscous fluids is homogenous and linear and the superposition principle can be used to obtain solutions for complex situations [13]. According to Shah and London [1], Lundberg et al. [14,15] solved this problem for the four fundamental types of boundary conditions in doubly connected ducts when the fluid is Newtonian.

Research on heat transfer in the presence of viscous dissipation is scarcer. For Newtonian fully developed pipe and channel flows, analytical solutions were obtained by Brinkman [16] and Ou and Cheng [17]. For power law fluids Toor [18] and Gill [19] presented analytical solutions for the Graetz problem and fully developed flow in pipes, respectively while Forrest and Wilkinson [20] added temperature effects in their numerical investigation of the Graetz pipe flow problem with constant wall temperature. Recently, Jambal et al. [21] investigated the effects of axial heat diffusion and viscous dissipation on the Graetz problem for power law fluids.

For axial flow inside an annulus most of the solutions are usually for rather limited conditions, such as with one insulated wall, no viscous dissipation or few thermal boundary conditions [22–29]. Exceptions are the works of Lin [30] and Jambal et al. [31] for power law fluids at constant wall temperature both accounting for viscous dissipation in their investigations of Couette-Poiseuille and annular flows, respectively. The recent analytical work of Coelho and Pinho [32] for Newtonian fluids also includes viscous dissipation for both constant wall temperatures and constant wall heat fluxes. The extensive investigations of Manglik and Fang [33] and Fang et al. [34] for flow of Newtonian and non-Newtonian fluids in concentric and eccentric annuli are again numerical and also do not account for viscous dissipation. In the extensive literature survey of Fang and Manglik [35] there is also no reference to work on concentric annular flow with viscoelastic fluids accounting for viscous dissipation.

Non-isothermal flows of viscoelastic fluids have capture the attention of researchers due to their industrial relevance. In particular, there have been significant contributions towards the development of accurate rheological constitutive and energy equations for viscoelastic fluids accounting for such effects as temperature dependent properties, compressibility and thermodynamics of non-equilibrium processes (Leonov [36,37], Wapperom and Hulsen [38], Peters and Baaijens [39], amongst others). A comprehensive review is presented in Wapperom [40].

Still, solutions are lacking for heat transfer in annular flows of highly viscoelastic fluids, including effects of viscous dissipation, for any combination of imposed heat fluxes or imposed temperatures at both walls for which this paper presents analytical solutions.

The paper is organized as follows: in Section 2 the general governing equations for non-isothermal viscoelastic flows are presented prior to their simplification. This leads to a fluid dynamical problem which is decoupled from the thermal problem and so the fully-developed hydrodynamic solution is presented. In Sections 3 and 4 the thermal energy equation is integrated and results presented for imposed wall heat fluxes and imposed wall temperatures, respectively. As alternatives to the very long analytical expressions for Nusselt numbers, we present in each Section compact formulae with coefficients listed in tables. For conciseness, the tables presented in the paper are limited, but the interested reader is invited to download an extensive set of Tables, as well as Fortran codes implementing the analytical solutions here derived, from the following internet address and under "heat transfer": http://www.fe.up.pt/~fpinho/research/menur.html.

2. Governing equations

The behaviour of viscoelastic fluids undergoing heat transfer processes is governed by the momentum, continuity and energy equations in addition to various constitutive equations for the stress, the heat flux and the internal energy. For non-isothermal flows the momentum and rheological constitutive equations are affected in two ways relative to an isothermal case: dependence of fluid properties on temperature and, on thermodynamic arguments the existence of extra terms in the constitutive equation [36,37], which can be traced back to the effect of temperature on the mechanisms acting at microscopic level. These changes, together with considerations of second law of thermodynamics for irreversible processes also affect the energy equation [38,41].

The analytical solutions are for dynamic and thermally fully-developed steady laminar flow in concentric annuli of Phan-Thien–Tanner fluids (PTT) having a zero second normal stress difference in pure shear flow. The annuli, shown schematically in Fig. 1(a), have inner and outer walls of radius R_i and R_o, respectively, defining the radius ratio $\kappa = R_i/R_o$ and annular gap $\delta = R_o - R_i$.

The constitutive equation adopted here for the PTT fluid is

$$f(\tau_{kk})\boldsymbol{\tau} + \lambda \overset{\nabla}{\boldsymbol{\tau}} - \lambda \dot{T} H_T \left(\boldsymbol{\tau} + \frac{\eta}{\lambda}\boldsymbol{I}\right) = 2\eta \boldsymbol{D} \tag{1}$$

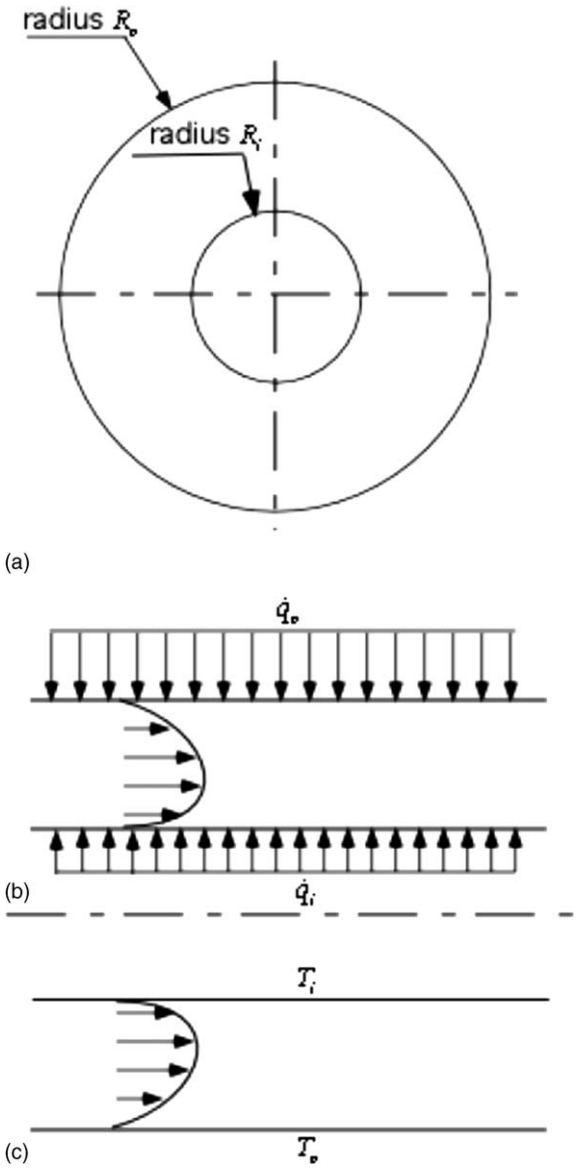

Fig. 1. Schematic representation of the annular geometry and of the axisymmetric thermal boundary conditions (BC). (a) Cross section; (b) upper half of annular duct: BC for imposed wall heat fluxes; (c) lower half of annular duct: BC imposed wall temperatures.

with a linear stress coefficient given by

$$f(\tau_{kk}) = 1 + \frac{\varepsilon\lambda}{\eta}\tau_{kk}. \tag{2}$$

In Eqs. (1) and (2) $\boldsymbol{D}$ is the deformation rate tensor ($\boldsymbol{D} = (\nabla \boldsymbol{u} + (\nabla \boldsymbol{u})^T)/2$) and the fluid properties are the relaxation time (λ), the viscosity coefficient (η) and a parameter limiting the extensional viscosity of the fluid (ε).$\overset{\nabla}{\tau}$ denotes Oldroyd's upper convective derivative of the stress tensor given in Eq. (3).

$$\overset{\nabla}{\boldsymbol{\tau}} = \frac{D\tau}{Dt} - \boldsymbol{\tau}.\nabla u - (\nabla u)^T.\boldsymbol{\tau} \tag{3}$$

The last term on the left-hand-side of Eq. (1) accounts for the variation with temperature of the connector force representing the fluid structure and appears when this equation is

derived from kinetic theory arguments. Its influence vanishes for isothermal flows ($\dot{T}=0$), but here we also neglect it following Peters and Baaijens [39]. In general, the relaxation time and the viscosity coefficient (and less so the extensibility coefficient) depend on temperature, especially for temperatures in the range $T_g < T < T_g + 100\,\mathrm{K}$, where T_g is the glass transition temperature. Such temperature dependence can be accounted for by an Arrehnius type of expression, as in the non-isothermal heat transfer investigation of Nikoleris and Darby [42] of differential viscoelastic fluids in rectangular ducts, or by invoking the time–temperature superposition principal [43]. Here we consider only temperature independent properties to allow analytical solutions to be obtained.

As a consequence of considering temperature independent properties, and of neglecting the $\lambda \dot{T} H_T$ term in the constitutive equation, the fluid dynamical problem becomes decoupled from the thermal problem and its solution identical to that for an isothermal flow. This fully-developed flow solution was obtained by Pinho and Oliveira [10], but for convenience we use the expressions of Cruz and Pinho [11] for the non-dimensional velocity and shear stress in Eqs. (4) and (7), respectively. For compactness, some non-dimensional quantities used here differ from the corresponding quantities in those two works, such as y^+ and y_*^+ defined below.

$$u^+ \equiv \frac{u}{U} = -2\Lambda \ln(Yy^+) - \frac{\varphi {y^+}^4}{{y_*^+}^4} + \frac{\Lambda {y^+}^2}{{y_*^+}^2} - \frac{2\varphi {y_*^+}^2}{{y^+}^2} + c_1 \tag{4}$$

Parameters c_1, Λ and φ are given by

$$\Lambda \equiv \frac{2X\kappa^2 {y_*^+}^2 (96X^2\varepsilon We^2\kappa^2 {y_*^+}^2 - \kappa^2 + 2\kappa - 1)}{(\kappa-1)^4} \quad \text{and}$$

$$\varphi \equiv \frac{32X^3\varepsilon We^2\kappa^4 {y_*^+}^4}{(\kappa-1)^4} \tag{5}$$

$$c_1 = -2\Lambda \ln(1-\kappa) + 2\varphi\kappa^2 {y_*^+}^2 - \frac{\Lambda}{\kappa^2 {y_*^+}^2} + \frac{\varphi}{\kappa^4 {y_*^+}^4} \tag{6}$$

$$\tau_{rx}^+ \equiv \frac{\tau_{rx}}{\eta^U/\delta} = 4Yy_*^+ X \left(\frac{y_*^+}{y^+} - \frac{y^+}{y_*^+} \right). \tag{7}$$

In these equations U represents the bulk velocity, X the ratio between a characteristic (U_c) and the bulk velocities ($X = U_c/U$) and We is the Weissenberg number based on the bulk velocity, and defined as $We = \lambda U/\delta$. The characteristic velocity U_c is a normalization of the constant pressure gradient ($p_{,x}$) defined as $U_c = -p_{,x}\delta^2/(8\eta)$. Y is a geometric parameter ($Y = \kappa/(1-\kappa)$), y^+ the radius (r) normalized by the inner cylinder radius ($y^+ = r/R_i = r/(\delta Y)$) and y_*^+ refers to the non-dimensional radial location of zero shear stress. For the PTT fluid, the ratio X and the zero shear stress radius (y_*^+) are given by Eqs. (16) and (23) in Pinho and Oliveira [10], respectively, and result from two cubic equations. However, our definition of y_*^+ differs from that of Pinho and Oliveira [10] (subscript PO) according to $y_*^+ = y_{*,\mathrm{PO}}^+ \delta/R_i = y_{*,\mathrm{PO}}^+ (1-\kappa)/\kappa$.

To compact the solution, we further define the following three parameters:

$$\beta = 16Bry_*^{+2} X^2 Y^4, \quad \Omega \equiv 32\varepsilon We^2 X^2 Y^2 y_*^{+2} \quad \text{and}$$

$$\Psi \equiv Y^2(1 + 8XBr) \tag{8}$$

The normalized shear rate appearing in the viscous dissipation term of the normalized energy equations in Sections 3 and 4 is calculated by

$$\frac{\mathrm{d}u^+}{\mathrm{d}y^+} = Y\tau_{rz}^+ (1 + 2\varepsilon We^2 \tau_{rz}^{+2}) \tag{9}$$

The general energy equation for an incompressible viscoelastic fluid modeled by the Phan-Thien–Tanner equation is presented by Peters and Baaijens [39], assuming that the internal energy not only depends on temperature but also on the strain, and is given by

$$-\vec{\nabla}.\boldsymbol{q} + \alpha\boldsymbol{\tau} : \boldsymbol{D} + (1-\alpha)\frac{\mathrm{tr}\boldsymbol{\tau}}{2\lambda}\left(1 + \frac{\varepsilon\lambda}{\eta}\mathrm{tr}\boldsymbol{\tau}\right) = \rho c_p \dot{\boldsymbol{T}} \tag{10a}$$

where the two last terms on the left-hand-side represent the mechanical energy supply by the viscoelastic medium. Term τ:$\boldsymbol{D}$, the viscous dissipation, accounts for the so-called entropic elasticity, which quantifies the energy that is stored as entropy and so contributes to temperature changes. The $(1-\alpha)$ term is the energy elasticity contribution and quantifies the energy stored elastically as internal energy which can be released later and therefore does not contribute to temperature changes. For the heat flux Fourier's law of heat conduction is assumed with an isotropic thermal conductivity ($q = -k\vec{\nabla}T$) so for this steady flow the energy equation to be solved reduces to

$$k\frac{1}{r}\frac{\partial}{\partial r}\left(r\frac{\partial T}{\partial r}\right) + \alpha\tau_{rx}\frac{\mathrm{d}u}{\mathrm{d}r} + (1-\alpha)\,\tau_{xx}\frac{(1+(\varepsilon\lambda/\eta)\tau_{xx})}{2\lambda} = \rho c_p u\frac{\partial T}{\partial x}, \tag{10b}$$

where the temperature T varies with the axial and radial coordinates, denoted x and r, respectively, k, ρ and c_p are the thermal conductivity, density and specific heat of the fluid, respectively. Variable u represents the axial velocity and τ_{xr} is the relevant shear stress. Normalization of this equation is problem-dependent and is deferred to Sections 3 and 4.

The split of mechanical energy into entropic elasticity and energetic elasticity is quantified by coefficient α, and depends on both the polymer and the flow type. Sarti and Esposito [44] experimentally showed that for melts of amorphous polymers, such as polyisobutylene and polyvinylacetate, $\alpha = 1$ provided the temperature is well above the glass transition temperature. The numerical simulations of Peters and Baaijens [39] of the non-isothermal flow around a confined cylinder have also shown that the temperature profiles for PTT fluids with $\alpha = 0$ and $\alpha = 1$ are fairly similar, although the differences increase with Weissenberg number, and both are considerably different from what is obtained for a purely viscous fluid with the same viscosity behaviour as that of the PTT. However, this is not an issue here because for fully-developed pure shear flow there is no internal energy storage, only viscous dissipation as shown in Wapperom

[40] and Wapperom and Hulsen [38]. This can be easily demonstrated here: regardless of the value of α it suffices to substitute τ_{xx} and du/dr in equation (10b) by the expressions of equations (8) and (10) in Pinho and Oliveira [10], respectively. The terms involving α cancel out and the final result is mathematically equivalent to setting $\alpha = 1$ in equation (10b).

For the energy equation two sets of boundary conditions will be investigated separately: (1) peripherally and axially constant heat fluxes at both walls (Fig. 1(b))

$$r = R_\mathrm{i} \rightarrow -k\frac{\partial T}{\partial r} = \dot{q}_\mathrm{i} \tag{11a}$$

$$r = R_\mathrm{o} \rightarrow T = T_\mathrm{o}(x) \tag{11b}$$

where the outer wall heat flux will be imposed later when calculating the streamwise derivative of the bulk temperature; (2) peripherally and axially constant wall temperatures (Fig. 1(c))

$$r = R_\mathrm{i} \rightarrow T = T_\mathrm{i} \tag{12a}$$

$$r = R_\mathrm{o} \rightarrow T = T_\mathrm{o} \tag{12b}$$

Note that in each case the boundary conditions are axisymmetric, but for conciseness in Fig. 1 we show a different set on each half annulus.

3. Solution for imposed uniform wall heat fluxes

3.1. Non-dimensional energy equation

For imposed uniform wall heat fluxes $\partial T/\partial x = \partial T_\mathrm{w}/\partial x = \partial \bar{T}/\partial x$ is a constant [13], with subscript w denoting a wall and the overbar denoting mass averaging. To make the energy equation non-dimensional for this problem, two different normalizations are used for the temperature. For the terms on the left-hand-side of Eq. (10b) the definition embodied in Eq. (13a) is used, based on the temperature at the outer wall ($T_\mathrm{o}(x)$), whereas for the right-hand-side of Eq. (10b) the above equality of the longitudinal temperature gradient is used together with the normalization of Eq. (13b), where T_in represents the inlet temperature.

$$T^+ \equiv \frac{T - T_\mathrm{o}}{2\delta\dot{q}/k} \tag{13a}$$

$$\bar{T}' \equiv \frac{\bar{T} - T_\mathrm{in}}{2\delta\dot{q}/k} \tag{13b}$$

The non-dimensional axial coordinate is $x' = 2x/(\delta Re\, Pr)$, the Reynolds and the Prandtl numbers are defined as $Re = \rho U 2\delta/\eta$ and $Pr = \eta c_p/k$, and the non-dimensional energy equation becomes

$$\frac{1}{y^+}\frac{\partial}{\partial y^+}\left(y^+\frac{\partial T^+}{\partial y^+}\right) + YBr\tau_{rx}^+\frac{\mathrm{d}u^+}{\mathrm{d}y^+} = Y^2 u^+\frac{\mathrm{d}\bar{T}'}{\mathrm{d}x'} \tag{14}$$

where the derivative on the right-hand-side is a constant and the Brinkman number is defined as

$$Br = \frac{\eta U^2}{2\delta\dot{q}} \tag{15}$$

This definition is adequate for arbitrarily imposed wall heat flux. However, the use of the perimeter-average wall heat flux $\dot{q}$ of Eq. (16), based on the inner ($\dot{q}_\mathrm{i}$) and outer ($\dot{q}_\mathrm{o}$) wall heat fluxes, turns Br into a quantity dependent on κ. This definition is not usual in the less general solutions in the literature and must be taken into account when performing comparisons. The perimeter-average wall heat flux is

$$\dot{q} = \frac{\dot{q}_\mathrm{i}R_\mathrm{i} + \dot{q}_\mathrm{o}R_\mathrm{o}}{R_\mathrm{i} + R_\mathrm{o}} = \dot{q}_\mathrm{i}\frac{\kappa + \Phi}{1 + \kappa} \tag{16}$$

where Φ stands for the ratio between the outer and inner wall heat fluxes, $\Phi \equiv \dot{q}_\mathrm{o}/\dot{q}_\mathrm{i}$.

The normalized heat flux boundary conditions of Eqs. (11a) and (11b) become

$$y^+ = y_i^+ = 1 \rightarrow \frac{\partial T^+}{\partial y^+} = \frac{\kappa(\kappa+1)}{2(\kappa+\Phi)(\kappa-1)} \tag{17a}$$

$$y^+ = y_\mathrm{o}^+ = \frac{1}{\kappa} \rightarrow T^+ = 0 \tag{17b}$$

The outer wall boundary condition (Eq. (17b)) is a consequence of the normalization used for temperature, c.f. Eq. (13a). Even though this is a problem with imposed heat flux at both walls, this is done at the outer wall via a temperature, Eq. (11b). This is so because the outer wall heat flux is indirectly imposed when the derivative on the right-hand-side of Eq. (14) is calculated from the following energy balance over a control volume encompassing the annulus and both walls:

$$\dot{q}_\mathrm{i}2\pi R_\mathrm{i}\mathrm{d}x + \dot{q}_\mathrm{o}2\pi R_\mathrm{o}\mathrm{d}x + U2\pi(R_\mathrm{i}|\tau_\mathrm{wi}| + R_\mathrm{o}|\tau_\mathrm{wo}|)\mathrm{d}x = \rho c_p U\pi(R_\mathrm{o}^2 - R_\mathrm{i}^2)\mathrm{d}\bar{T}. \tag{18}$$

Solving and normalizing Eq. (18) gives the following constant axial gradient of non-dimensional bulk temperature

$$\frac{\mathrm{d}\bar{T}'}{\mathrm{d}x'} = 1 + 8BrX. \tag{19}$$

Back-substitution in the non-dimensional energy Eq. (14) the final solution only contains a single definition of non-dimensional temperature (T^+), even for the bulk temperature ($\bar{T}^+$) expression in Section 3.2.

3.2. Analytical solution

Integration of the energy equation was carried out with the help of the symbolic mathematics code Derive 5 from Texas Instruments.

The heat transfer from the walls to the fluid is quantified via the inner wall (Nu_i) and outer wall (Nu_o) Nusselt numbers. Each Nusselt number is defined as $Nu = 2\delta h/k$, i.e. on the basis of the hydraulic diameter ($D_\mathrm{H} = 2\delta$) and the heat transfer coefficient at that wall (h), calculated from $\dot{q}_\mathrm{w} = h(T_\mathrm{w} - \bar{T})$. Normalising temperatures by Eq. (13a), the Nusselt number becomes $Nu_\mathrm{w} = \dot{q}_\mathrm{w}/[\dot{q}(T_\mathrm{w}^+ - \bar{T}^+)]$, and after using Eq. (16), the following expressions are obtained:

-at the inner wall, $$Nu_\mathrm{i} = \frac{(1+\kappa)}{(\kappa+\Phi)}\frac{1}{(T_\mathrm{i}^+ - \bar{T}^+)} \tag{20a}$$

-at the outer wall, $$Nu_o = \frac{\Phi(1+\kappa)}{(\kappa+\Phi)}\frac{1}{(T_o^+ - \bar{T}^+)} \quad (20b)$$

The inner wall temperature is calculated from the derived temperature profile whereas the outer wall non-dimensional temperature is fixed at $T_o^+ = 0$. Finally, the normalised bulk temperature is the following integration of the temperature profile

$$\bar{T}^+ = \int_{y_i^+}^{y_o^+} 2\frac{\kappa^2}{1-\kappa^2} u^+ T^+ y^+ \mathrm{d}y^+ \quad (21)$$

The analytical solution for the temperature profile, the bulk temperature and the inner wall temperature are given by Eqs. (22), (25) and (26), below.

- Non-dimensional temperature profile, $T^+(y^+)$

$$T^+ = \frac{y_*^{+2}[\beta(4\Omega-1)-2\varphi\Psi]}{2}(\ln y^+)^2 + \frac{\Lambda\Psi y^{+2}}{2}\ln\left(\frac{1}{y^+}\right) - \frac{y^{+6}(\varphi\Psi+\Omega\beta)}{36y_*^{+4}} - \frac{\Omega\beta y_*^{+4}}{4y^{+2}} + \frac{y^{+4}[\Lambda\Psi+\beta(4\Omega-1)]}{16y_*^{+2}} + \frac{y^{+2}(2\Lambda\Psi-6\Omega\beta+\Psi c_1+2\beta)}{4} + c_2 + c_3 \quad (22)$$

where the constants of integration are given by

$$c_2 = \Lambda\Psi\ln Y + \frac{\varphi\Psi+\beta\Omega}{6y_*^{+4}} - \frac{\Lambda\Psi+\beta\Omega(y_*^{+4}-6)+\Psi c_1+2\beta-1}{2} - \frac{\Lambda\Psi+\beta(4\Omega-1)}{4y_*^{+2}} + \frac{\Phi(1-\Phi)}{2(\Phi+1)(\kappa+\Phi)} + \frac{1}{(\Phi+1)(\kappa-1)} \quad (23)$$

$$c_3 = -\Lambda\Psi\ln(1-\kappa)\left(\ln\kappa+\frac{1}{2\kappa^2}\right) + (\ln\kappa)^2\left[\Psi(\varphi y_*^{+2}+\Lambda)+\frac{\beta y_*^{+2}(1-4\Omega)}{2}\right] + \frac{\ln\kappa}{6y_*^{+4}}(\beta\Omega+\varphi\Psi) - \frac{\ln\kappa}{2}[\beta\Omega(y_*^{+4}-6)+\Psi(\Lambda+c_1) + 2\beta-1] - \frac{\Lambda\Psi+\beta(4\Omega-1)}{4y_*^{+2}}\ln\kappa + \frac{\varphi\Psi+\beta\Omega}{36\kappa^6 y_*^{+4}} + \frac{\beta\Omega\kappa^2 y_*^{+4}}{4} + \frac{\Phi(1-\Phi)\ln\kappa}{2(\Phi+1)(\kappa+\Phi)} + \frac{\ln\kappa}{(\Phi+1)(\kappa-1)} - \frac{\Psi(2\Lambda+c_1)+2\beta(1-3\Omega)}{4\kappa^2} - \frac{\Lambda\Psi+\beta(4\Omega-1)}{16\kappa^4 y_*^{+2}} \quad (24)$$

- Inner wall temperature, T_i^+

$$T_i^+ = \frac{\Lambda\Psi}{2}\ln\left(\frac{1}{Y}\right) - \frac{\beta[4\Omega(9y_*^{+8}+54y_*^{+4}-9y_*^{+2}+1)-9y_*^{+2}(8y_*^{+2}-1)]+4\varphi\Psi}{144y_*^{+2}} + \frac{\Psi c_1}{4} + \frac{\Lambda\Psi(8y_*^{+2}+1)}{16y_*^{+2}} + c_3 \quad (25)$$

- Bulk temperature, $\bar{T}^+$

$$\bar{T}^+ = A_1[\ln(1-\kappa)]^2 + A_2\ln(1-\kappa) + B_1(\ln\kappa)^3 + B_2(\ln\kappa)^2 + B_3\ln\kappa + B_4 \quad (26)$$

where the coefficients A and B are presented in Appendix A.

This general analytical solution has various particular cases, several of which have been obtained previously and used here to check the validity of this solution: (i) the channel flow, with identical wall heat fluxes and viscous dissipation of Oliveira and Pinho [45]; (ii) the pipe flow, with viscous dissipation, of Oliveira and Pinho [45], (iii) the channel flow case of Shah and London [1] (their Eq. 273) without viscous dissipation.

The Nusselt numbers are given in Eqs. (20a) and (20b) upon substitution of the above expression for the wall and bulk temperatures. Since the Nusselt numbers are used more often in engineering calculations, it is advantageous to have more compact expressions. Specifying numerical values for the radius ratio, such compact exact expressions are given in Eqs. (28a) and (28b) for the inner and outer walls Nusselt numbers, respectively:

$$Nu_i = \frac{\alpha_1}{Br((\Phi/\kappa)+1)+\alpha_2\Phi+\alpha_3} \quad (28a)$$

$$Nu_o = \frac{B_1\Phi}{Br((\Phi/\kappa)+1)+\beta_2\Phi+\beta_3} \quad (28b)$$

where the coefficients α_i and β_i depend on the radius ratio and εWe^2. Values of these coefficients are listed in Table 1 for a limited number of cases. Full sets of Tables are freely available from the internet (at http://www.fe.up.pt/~fpinho/research/menur.html and under "heat transfer") together with Fortran codes implementing the exact equations derived here. Also, see [32] for the limit of $\varepsilon We^2 \to 0$.

A particularly interesting case, obtained from the general solution, corresponds to heating or cooling at both walls leading to identical wall temperatures ($T_i^+ = T_o^+$). This takes place for a heat flux ratio of

$$\Phi_c = \frac{72\kappa^7 y_*^{+4}(\kappa+1)\ln\kappa}{(\kappa-1)\{J_1 - J_2(\ln\kappa)^2 + J_3\ln\kappa + J_4\}} - \kappa \quad (29)$$

where $J_1 = 72\Lambda\Psi\kappa^4 y_*^{+4}\ln(1-\kappa)(2\kappa^2\ln\kappa-\kappa^2+1)$, $J_2 = 72\kappa^6 y_*^{+4}[y_*^{+2}B_{11}+2\Lambda\Psi]$, $J_3 = 12\kappa^6\{6\Omega\beta y_*^{+8}+6y_*^{+4}[\Psi(2\Lambda+c_1)-6\Omega\beta+2\beta]+3y_*^{+2}[\Lambda\Psi+\beta(4\Omega-1)]-2(\varphi\Psi+\Omega\beta)\}$ and $J_4 = (1-\kappa^2)\{36\Omega\beta\kappa^6 y_*^{+8}+36\kappa^4 y_*^{+4}[(2\Lambda+c_1)\Psi-2\beta(3\Omega-1)]+9\kappa^2 y_*^{+2}S_1[\Lambda\Psi+\beta(4\Omega-1)]-4S_2(\varphi\Psi+\Omega\beta)\}$. B_{11}, S_1 and S_2 are defined in Appendix A.

Table 1
Coefficients for the Nusselt number Eqs. (28a) and (28b)

κ	α_1	α_2	α_3	β_1	β_2	β_3
(a) $\varepsilon We^2 = 0.1$						
0.02	686.53	−93.522	20.786	95.892	20.100	−0.26125
0.05	105.37	−13.809	5.8340	41.556	8.6148	−0.27228
0.1	40.478	−5.0222	3.3421	22.859	4.6958	−0.28361
0.2	18.507	−2.0906	2.1355	13.177	2.6755	−0.29770
0.3	12.479	−1.2978	1.6890	9.8451	1.9771	−0.30717
0.4	9.6938	−0.93506	1.4432	8.1475	1.6169	−0.31436
0.5	8.0933	−0.72822	1.2838	7.1171	1.3946	−0.32019
0.6	7.0547	−0.59493	1.1705	6.4254	1.2422	−0.32512
0.7	6.3259	−0.50202	1.0853	5.9297	1.1305	−0.32940
0.8	5.7861	−0.43363	1.0185	5.5577	1.0445	−0.33321
0.9	5.3698	−0.38123	0.96448	5.2689	0.97599	−0.33666
1	5.0387	−0.33984	0.91983	5.0387	0.91983	−0.33984
(b) $\varepsilon We^2 = 10$						
0.02	−3868.4	520.16	−118.23	345.12	68.611	−0.92813
0.05	845.48	−110.77	47.214	148.47	29.369	−0.97256
0.1	217.13	−27.235	18.045	81.446	16.069	−1.0216
0.2	83.196	−9.5981	9.6268	47.088	9.2575	−1.0865
0.3	52.535	−5.6060	7.1094	35.383	6.9163	−1.1327
0.4	39.352	−3.9046	5.8437	29.472	5.7144	−1.1697
0.5	32.088	−2.9742	5.0663	25.915	4.9755	−1.2010
0.6	27.505	−2.3915	4.5345	23.550	4.4714	−1.2286
0.7	24.355	−1.9938	4.1451	21.874	4.1034	−1.2535
0.8	22.058	−1.7059	3.8463	20.631	3.8215	−1.2764
0.9	20.310	−1.4881	3.6089	19.680	3.5978	−1.2978
1	18.934	−1.3180	3.4154	18.934	3.4154	−1.3180

3.3. Discussion of results

In the general case of imposed uniform wall heat fluxes, these are positive when heating the fluid and negative when cooling. For wall heating or cooling at both walls, the heat flux ratio is positive whereas the Brinkman number, Eq. (15), changes sign from positive for the former to negative for the latter. We restrict our discussion to $Br > 0$, $\Phi > 0$ and a radius ratio (κ) of 0.5.

In Fig. 2, the inner wall Nusselt number is plotted as a function of Br, εWe^2 and Φ. The three values of Φ selected correspond to three different situations: for $\Phi = 0.01$ inner wall heating is so large compared to outer wall heating that the thermal behaviour corresponds to that of an insulated outer wall and is identical to that for $\Phi \leq 0.01$; for $\Phi \geq 100$ the thermal behaviour is akin to that for an insulated outer wall and is well represented by the curves for $\Phi = 100$; In between these two values the fluxes at both walls are important to determine the thermal characteristics of the flow and this case is represented here by $\Phi = 1$.

Regardless of the heat flux ratio the Nusselt number increases with εWe^2 for two reasons: (1) the velocity profiles become steeper near the walls (c.f. Figs. 3 and 6 in [10]), increasing the proportion of fluid flowing near the walls, which contributes to a reduction of the overall thermal resistance; (2) higher values of εWe^2 increase shear-thinning, thus reducing the viscosity and by implication the internal heat generation (c.f. the variations of X or fRe in Figs. 1 and 7 of [10]), thus reducing the temperature difference $T_i^+ - \bar{T}$, as seen in Fig. 3.

Regarding the effect of the Brinkman number, the Nusselt number decreases with viscous dissipation, exactly because of the opposite effect. As internal heat generation becomes more important, the fluid heats more, especially near to the wall, and the difference between the wall and bulk temperatures increases (for example, compare the curves for $Br = 0.01$ and 1 in Fig. 3 at $\varepsilon We^2 = 0.01$). Since the wall heat flux remains constant, the heat transfer coefficient (Nusselt number) must necessarily decrease. Exceptions to this behaviour, also known to occur with Newtonian fluids, happen when the difference between the wall and bulk temperatures goes through zero and changes sign, leading to a singularity in the Nu_i profiles, as shown in Fig. 2(c)). This happens because of the heating effect of the other wall, together with the influence of the extra heat generated by viscous dissipation interfering with the relative magnitudes of bulk and wall temperatures, since the bulk temperature comes to exceed the wall temperature. This change in the relative magnitudes of the wall and bulk temperatures is shown in the temperature profiles of Fig. 3, especially Fig. 3(c)), which also illustrates the different behaviors for small and large amounts of viscous dissipation: when viscous dissipation is weak the fluid and bulk temperatures are everywhere limited by the two wall temperatures, but as Br increases those temperatures exceed the limiting values.

For the outer Nusselt number the trends are similar, but reversed relative to the heat flux ratio: there are smooth variations of Nu_o at large values of Φ and the singularities due to a change of sign in temperature difference appear at low Φ. The thermal behaviour for other combinations of Φ, Br, εWe^2 and κ can also be explained on the basis of similar physical arguments.

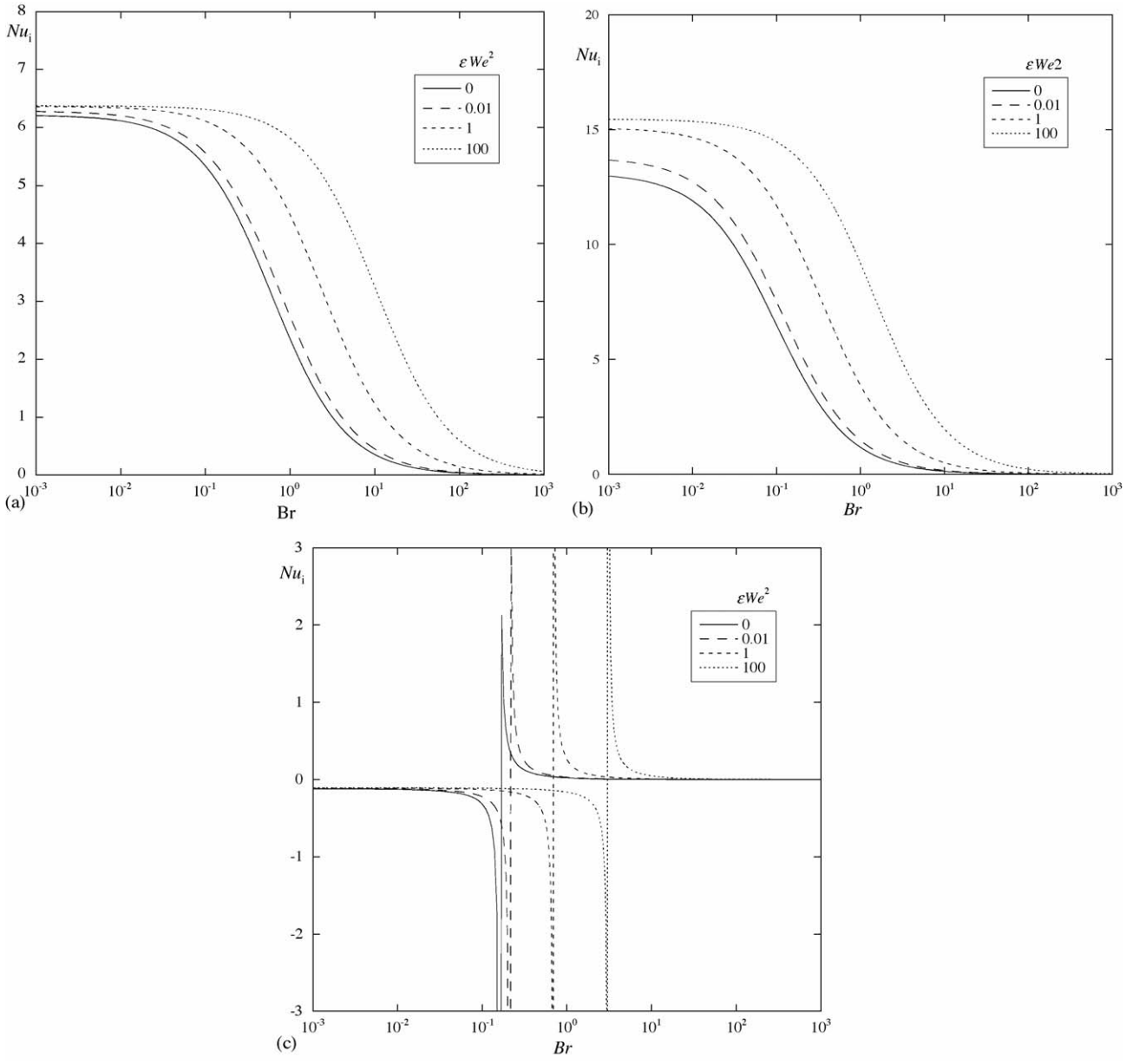

Fig. 2. Variation of the inner wall Nusselt number with the Brinkman number ($Br>0$) and εWe^2 for $\kappa=0.5$. (a) $\dot{q}_o/\dot{q}_i = 0.01$; (b) $\dot{q}_o/\dot{q}_i = 1$; (c) $\dot{q}_o/\dot{q}_i = 100$.

4. Solution for imposed uniform temperatures at walls

4.1. Non-dimensional energy equation

Two different normalizations are used for temperature since it is advantageous to distinguish between the situations of different and identical wall temperatures, and the non-dimensional temperatures to be used in the energy equation (T^*) are defined in Eqs. (30a) and (30b), respectively.

$$T^* = \frac{T - T_i}{T_o - T_i}, \quad \text{when } T_i \neq T_o \tag{30a}$$

$$T^* = \frac{T - T_{in}}{T_w - T_{in}} \quad \text{when } T_w = T_i = T_o \tag{30b}$$

Only the asymptotic solution, for which $\partial\bar{T}/\partial x = 0$, will be presented here. Upon substitution of the shear rate and shear stress expressions, the non-dimensional energy Eq. (10b) becomes

$$\frac{1}{y^+}\frac{\partial}{\partial y^+}\left(y^+\frac{\partial T^*}{\partial y^+}\right) = -\beta\left(\frac{y_*^+}{y^+} - \frac{y^+}{y_*^+}\right)^2\left[1 + \Omega\left(\frac{y_*^+}{y^+} - \frac{y^+}{y_*^+}\right)^2\right] \tag{31}$$

The boundary conditions and the Brinkman number are also different for the two cases, as follows:

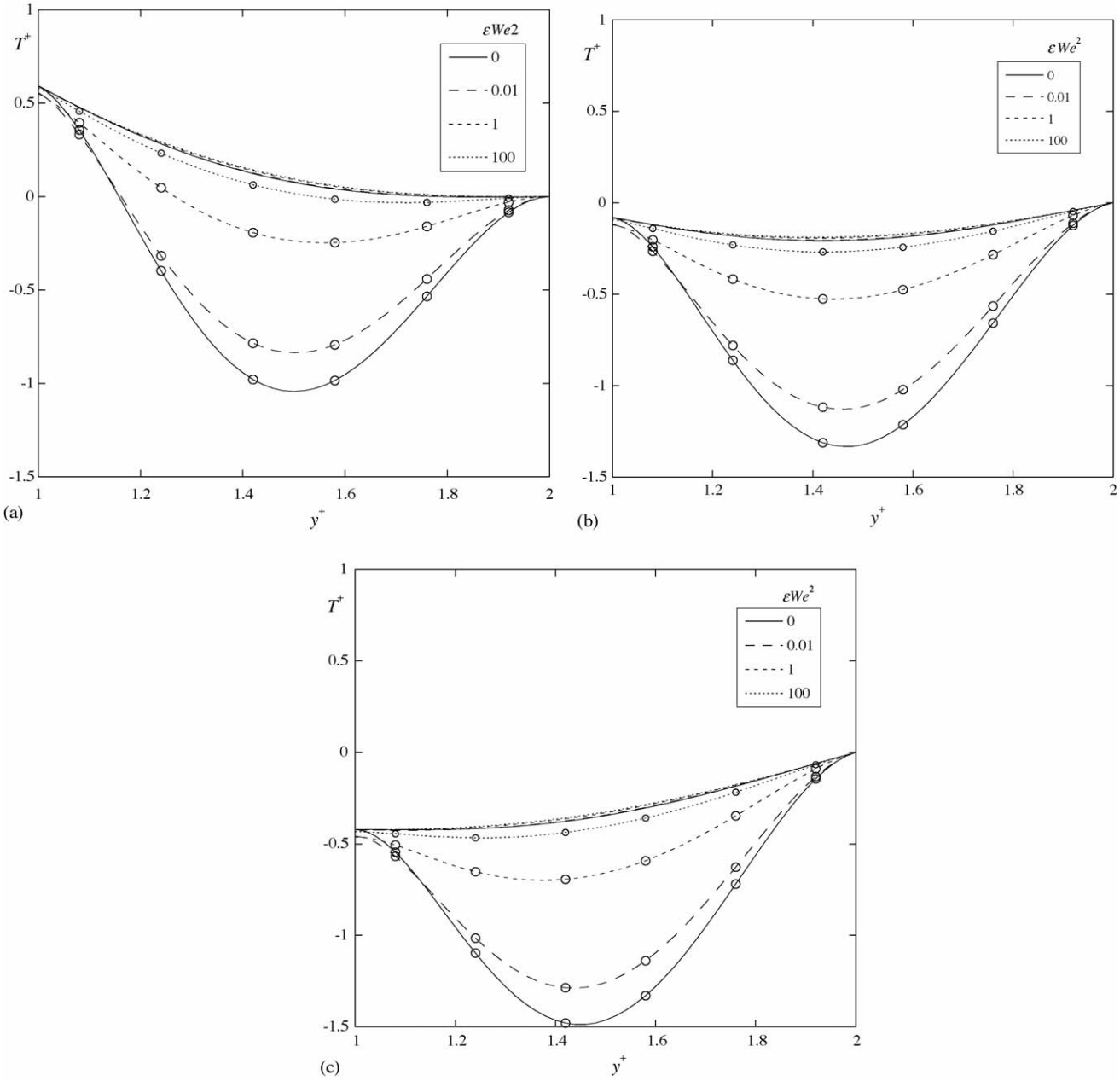

Fig. 3. Temperature variation across a $\kappa = 0.5$ annulus as a function of εWe^2 for $Br = 0.01$ (no symbols) and $Br = 1$ (O). (a) $\dot{q}_o/\dot{q}_i = 0.01$; (b) $\dot{q}_o/\dot{q}_i = 1$; (c) $\dot{q}_o/\dot{q}_i = 100$.

(1) $T_o \neq T_i$

inner wall : $y^+ = 1 \rightarrow T_i^* = 0$; outer wall :

$$y^+ = \frac{1}{\kappa} \rightarrow T_o^* = 1 \tag{32}$$

$$Br = \frac{\eta U^2}{k(T_o - T_i)} \tag{33}$$

For this case, when setting $\varepsilon We^2 = 0$ the Newtonian solution of Coelho and Pinho [32] is recovered and further setting $Br = 0$ provides the solution of Shah and London [1] as it should be. Setting $Br \rightarrow \infty$ we get the same solution as for identical wall temperatures and for which both the inner and outer wall Nusselt numbers are independent of Br.

(2) $T_w = T_o = T_i$,

$$Br = \frac{\eta U^2}{k(T_w - T_{in})} \tag{34}$$

inner wall : $y^+ = 1 \rightarrow T_i^* = 1$;

$$\text{outer wall} : y^+ = \frac{1}{\kappa} \rightarrow T_o^* = 1 \tag{35}$$

4.2. Analytical solution

The Nusselt numbers at the inner and outer walls are now defined in Eqs. (36a) and (36b), respectively.

$$Nu_\mathrm{i} = -\frac{2}{Y}\frac{\mathrm{d}T^*/\mathrm{d}y^+\big|_{y^+=1}}{T_\mathrm{i}^* - \bar{T}^*} \tag{36a}$$

$$Nu_\mathrm{o} = \frac{2}{Y}\frac{\mathrm{d}T^*/\mathrm{d}y^+\big|_{y^+=1/\kappa}}{T_\mathrm{o}^* - \bar{T}^*} \tag{36b}$$

The bulk temperature is calculated as in Eq. (21), except for the use of the different non-dimensional temperature, i.e.

$$\bar{T}^* = \int_{y_\mathrm{i}^+}^{y_\mathrm{o}^+} 2\frac{\kappa^2}{1-\kappa^2} u^+ T^* y^+ \,\mathrm{d}y^+ \tag{37}$$

The analytical solution for all the relevant quantities is given by Eqs. (38)–(45). Except for the constants of integration c_4 and c_5, and the above definitions of normalized temperature, Brinkman number and inner wall temperature, the equations are the same regardless of whether the two wall temperatures are identical or different.

- Non-dimensional temperature profile, T^*

$$T^* = \frac{\beta y_*^{+^2}(4\Omega-1)(\ln y)^2 - \beta y^{+^2}(3\Omega-1)}{2} - \frac{\Omega\beta y_*^{+^4}}{4y^{+^2}} + \frac{\beta y^{+^4}(4\Omega-1)}{16 y_*^{+^2}} - \frac{\Omega\beta y^{+6}}{36 y_*^{+^4}} + c_4 \ln y + c_5 \tag{38}$$

with the constants of integration c_4 and c_5 given by Eqs. (39) and (40) for $T_\mathrm{i} \neq T_\mathrm{o}$ and Eqs. (41) and (42) for $T_\mathrm{i} = T_\mathrm{o}$.

$$c_4 = \frac{\beta y_*^{+^2}(4\Omega-1)\ln\kappa}{2} + \frac{\Omega\beta y_*^{+^4}(1-\kappa^2)}{4\ln\kappa} + \frac{\beta(1-\kappa^4)(4\Omega-1)}{16\kappa^4 y_*^{+^2}\ln\kappa} + \frac{\Omega\beta(\kappa^6-1)}{36\kappa^6 y_*^{+^4}\ln\kappa} + \frac{\beta(3\Omega-1)(\kappa^2-1)-2\kappa^2}{2\kappa^2\ln\kappa} \tag{39}$$

$$c_5 = \frac{\Omega\beta y_*^{+^4}}{4} + \frac{\beta(1-4\Omega)}{16 y_*^{+^2}} + \frac{\Omega\beta}{36 y_*^{+^4}} + \frac{\beta(3\Omega-1)}{2} \tag{40}$$

$$c_4 = \frac{\beta y_*^{+^2}(4\Omega-1)\ln\kappa}{2} + \frac{\Omega\beta y_*^{+^4}(1-\kappa^2)}{4\ln\kappa} + \frac{\beta(1-\kappa^4)(4\Omega-1)}{16\kappa^4 y_*^{+^2}\ln\kappa} + \frac{\Omega\beta(\kappa^6-1)}{36\kappa^6 y_*^{+^4}\ln\kappa} + \frac{\beta(3\Omega-1)(\kappa^2-1)}{2\kappa^2\ln\kappa} \tag{41}$$

$$c_5 = \frac{\Omega\beta y_*^{+^4}}{4} + \frac{\beta(1-4\Omega)}{16 y_*^{+^2}} + \frac{\Omega\beta}{36 y_*^{+^4}} + \frac{\beta(3\Omega-1)}{2} + 1 \tag{42}$$

The Nusselt numbers are calculated using Eqs. (36a) and (36b) with the temperature derivatives given by Eqs. (43) and (44).

-Derivative of temperature at inner wall, $\mathrm{d}T^*/\mathrm{d}y^+\big|_{y^+=1}$

$$\left.\frac{\mathrm{d}T^*}{\mathrm{d}y^+}\right|_{y^+=1} = c_4 + \frac{\Omega\beta y_*^{+^4}}{2} + \frac{\beta(4\Omega-1)}{4y_*^{+2}} - \frac{\Omega\beta}{6y_*^{+^4}} - \beta(3\Omega-1) \tag{43}$$

- Derivative of temperature at outer wall, $\mathrm{d}T^*/\mathrm{d}y^+\big|_{y^+=\frac{1}{\kappa}}$

$$\left.\frac{\mathrm{d}T^*}{\mathrm{d}y^+}\right|_{y^+=\frac{1}{\kappa}} = \beta(1-4\Omega)\left(\kappa y_*^{+^2}\ln\kappa - \frac{1}{4\kappa^3 y_*^{+^2}}\right) + c_4\kappa + \Omega\beta\left(\frac{\kappa^3 y_*^{+^4}}{2} - \frac{1}{6\kappa^5 y_*^{+^4}}\right) - \frac{\beta(3\Omega-1)}{\kappa} \tag{44}$$

- Bulk temperature, $\bar{T}^*$

$$\bar{T}^* = [D_1(\ln\kappa)^2 + D_2\ln\kappa + D_3]\ln(1-\kappa) + D_4(\ln\kappa)^3 + D_5(\ln\kappa)^2 + D_6\ln\kappa + D_7 \tag{45}$$

with expressions for coefficients D_1 to D_7 presented in Appendix A.

For ease of use, we also provide in Eqs. (46) and (47) compact expressions for the Nusselt numbers at the inner and outer walls, respectively, as a function of the Brinkman number. When $T_\mathrm{i} = T_\mathrm{o}$, $Nu_\mathrm{i} = \chi_1$ and $Nu_\mathrm{o} = \varepsilon_1$. The corresponding coefficients depend on the radius ratio and εWe^2 and are listed in Table 2 for a limited number of cases. Again, full sets of Tables together with Fortran codes implementing the exact equations derived here are freely available from the internet (at http://www.fe.up.pt/~fpinho/research/menur.html and under "heat transfer"). Also, see [32] for the limit of $\varepsilon We^2 \to 0$.

$$Nu_\mathrm{i} = \frac{\chi_1\, Br + \chi_2}{Br + \chi_3} \tag{46}$$

$$Nu_\mathrm{o} = \frac{\varepsilon_1\, Br + \varepsilon_2}{Br + \varepsilon_3} \tag{47}$$

4.3. Discussion of results

The discussion of these results is restricted to different wall temperatures ($T_\mathrm{i} \neq T_\mathrm{o}$), positive Brinkman numbers ($T_\mathrm{o} > T_\mathrm{i}$ according to definition in Eq. (33)) and two different radius ratios in Figs. 4 and 5 for the temperature profiles and the inner wall Nusselt numbers, respectively. In terms of heat fluxes, two different situations may occur as shown in the temperature profiles of Fig. 4: for low values of Br fluid heats at the warmer wall and cools at the colder wall, whereas for intense viscous dissipation the internal generation of heat increases the fluid temperature above the higher wall temperature and the fluid cools at both walls. The critical Brinkman number separating these two thermal conditions corresponds to the warmer wall behaving as an insulated wall, i.e. $\mathrm{d}T^*/\mathrm{d}y^+\big|_\mathrm{wall} = 0$ to be obtained from Eq.

Table 2
Coefficients for the Nusselt number Eqs. (46) and (47)

κ	χ_1	χ_2	χ_3	ε_1	ε_2	ε_2
(a) $\varepsilon We^2 = 0.1$						
0	–	–	–	11.041	0	0
0.02	103.80	78.105	2.5776	14.031	−1.5621	−0.54024
0.05	64.878	41.354	2.5606	14.822	−2.0677	−0.69961
0.1	46.555	26.284	2.4963	15.556	−2.6284	−0.86605
0.2	34.536	17.167	2.3687	16.513	−3.4334	−1.0850
0.3	29.620	13.562	2.2587	17.250	−4.0685	−1.2402
0.4	26.858	11.542	2.1637	17.891	−4.6168	−1.3616
0.5	25.062	10.220	2.0808	18.477	−5.1098	−1.4610
0.6	23.788	9.2720	2.0076	19.024	−5.5632	−1.5447
0.7	22.832	8.5524	1.9424	19.543	−5.9867	−1.6164
0.8	22.084	7.9829	1.8838	20.040	−6.3863	−1.6789
0.9	21.480	7.5183	1.8308	20.518	−6.7665	−1.7338
1	20.981	7.1303	1.7826	20.981	−7.1303	−1.7826
(b) $\varepsilon We^2 = 10$						
0	–	–	–	12.890	0	0
0.02	98.294	331.76	11.032	16.204	−6.6351	−2.2113
0.05	64.566	178.01	11.107	17.228	−8.9004	−2.9267
0.1	48.432	114.70	10.970	18.191	−11.470	−3.7016
0.2	37.490	75.924	10.537	19.386	−15.185	−4.7372
0.3	32.853	60.366	10.102	20.254	−18.110	−5.4724
0.4	30.187	51.563	9.7033	20.982	−20.625	−6.0456
0.5	28.422	45.754	9.3444	21.630	−22.877	−6.5127
0.6	27.153	41.568	9.0215	22.225	−24.941	−6.9040
0.7	26.189	38.373	8.7299	22.781	−26.861	−7.2380
0.8	25.428	35.835	8.4655	23.308	−28.668	−7.5272
0.9	24.809	33.758	8.2248	23.810	−30.382	−7.7805
1	24.293	32.018	8.0044	24.293	−32.018	−8.0044

(43) when $T_i > T_o$ and from Eq. (44) when $T_i < T_o$. Note here the essential use of dimensional temperatures.

The Nusselt number behaviour, for this condition of imposed wall temperature, is rather different from that in Section 3 for imposed wall heat fluxes, as shown by a direct comparison between Figs. 2 and 5, respectively. The heat flux at walls in Fig. 5 have two contributions in this limiting thermal flow condition: one contribution from the wall temperature difference (pure diffusion in an annulus), which is independent of εWe^2 and Br and only depends on κ and the contribution due to the internal heat generation, which is strongly dependent on Br and εWe^2. Since $Br > 0$ ($T_o > T_i$) the variations of Nu_i are monotonic with both Br and κ because the inner wall is always cooling the fluid (c.f. Fig. 5), with Nu_i increasing with the former and decreasing with the latter. Higher values of Br mean that more heat is generated internally and needs to be evacuated, leading to higher heat transfer coefficients and hence higher Nu_i. This is seen in all curves of Fig. 4.

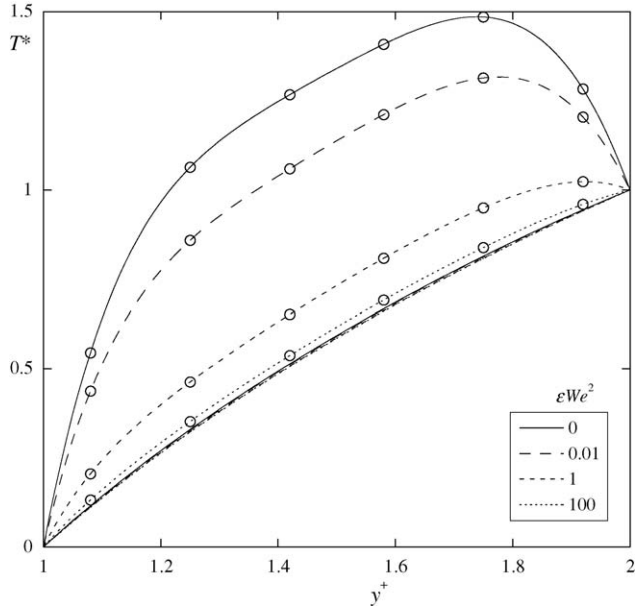

Fig. 4. Temperature profile T^* across the annulus ($\kappa = 0.5$) for $Br = +0.01$ (no symbols) and $Br = +1$ (◯) as a function of εWe^2.

The role of fluid rheology on Nu_i is more complex, because εWe^2 effects are coupled to viscous dissipative effects, leading to opposite behaviours at negligible and large Brinkman numbers, as can also be seen in Fig. 5. When viscous dissipation is weak, an increase in εWe^2 decreases Nu_i because the increased shear-thinning of the fluids actually results in less viscous dissipation than for a Newtonian fluid due to the lower viscosity of the former fluid, as already discussed in Section 3.3. So, when comparing cases for low and high values of εWe^2, the total wall heat flux (the temperature derivative in Eqs. (36a) and (36b)) will be lower for the latter case because of the lower total internal heat generation. However, as shear-thinning increases, the internal heat generation becomes more localized near the walls,

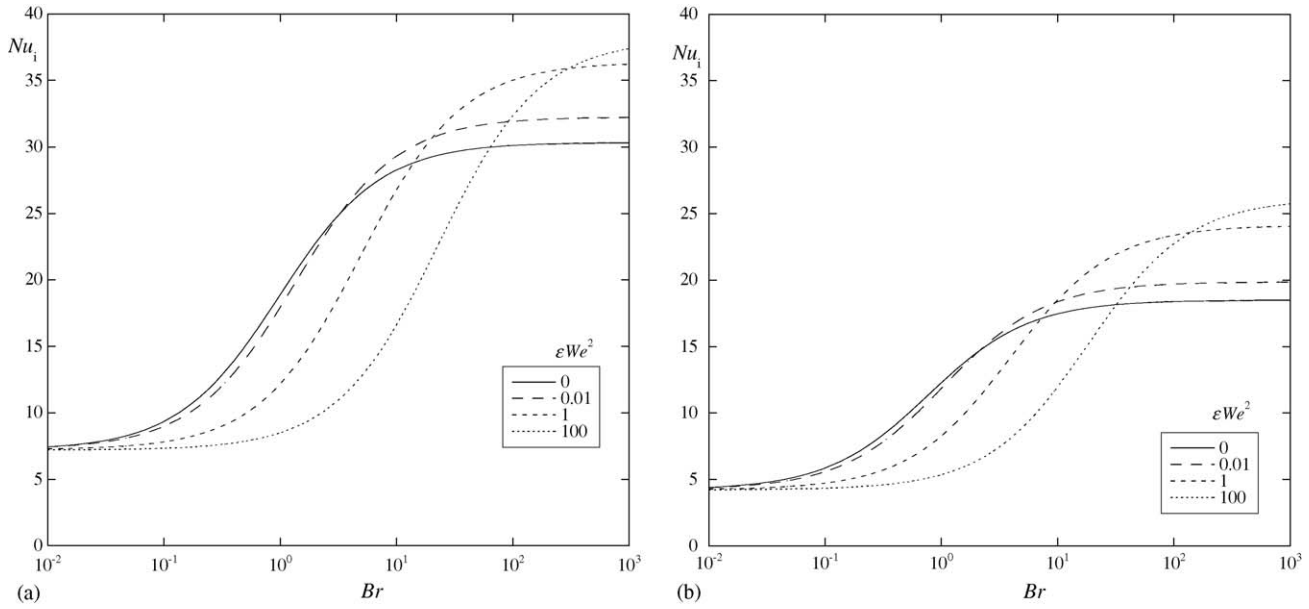

Fig. 5. Variation of the inner wall Nusselt number with the Brinkman number ($Br>0$) and εWe^2: (a) $\kappa=0.2$; (b) $\kappa=0.8$.

because of the correspondingly steeper velocity profiles. This reduces the thermal resistance and hence the difference between the wall and bulk temperatures, which appears in the denominator of Eqs. (36a and 36b). When Br is low, the decrease in wall heat flux is actually stronger than the decrease in the temperature difference, but for higher values of Br the magnitude of these effects of εWe^2 are reversed and the decrease in the temperature difference exceeds the decrease of the wall heat flux leading to higher Nusselt numbers for the more shear-thinning fluids.

For compactness no other plots were drawn, but if the magnitudes of the dimensional wall temperatures were to be reversed, i.e. $T_o<T_i$, the Brinkman number would become negative and the variations of Nu_i would no longer be monotonic, because below a critical negative Br (more negative Br) the fluid temperatures near the inner wall would be higher than the inner wall temperature and the heat flux would switch from heating to cooling, i.e. exactly the same behaviour observed near the outer wall in Fig. 4, now taking place at the inner wall. This also happens for Newtonian fluids [32], and the difference here is that the singularity appearing when $T_i=\bar{T}$ is εWe^2-dependent. Hence, we may also conclude that the behaviour of the outer wall Nusselt number (not shown) is qualitatively similar to that for Nu_i but reversed as far as the effect of Br is concerned: Nu_o varies monotonically for $Br<0$ and exhibits singularities for $Br>0$.

5. Conclusions

Analytical solutions are presented for fully-developed laminar convective heat transfer in concentric annuli of viscoelastic fluids modeled by the PTT equation with linear stress coefficient. The solutions account for internal heat generation due to viscous dissipation, but the fluid properties are assumed independent of temperature. The investigated boundary conditions were imposed uniform wall heat fluxes and imposed uniform wall temperatures.

The results are presented as explicit equations for the temperature profile, the inner and outer wall temperatures, the mixing temperature and, through their definitions for the inner and outer Nusselt numbers, as a function of the Brinkman number, the radius ratio, εWe^2 and, for the case with imposed wall fluxes, the wall heat flux ratio. For imposed wall temperatures, a solution is also given for the special case of identical wall temperatures, which cannot be used for $Br=0$. The variations of the inner and outer Nusselt numbers, as a function of all the independent parameters are discussed in Sections 3.3 and 4.3.

Although explicit, the equations are rather long, so that, for ease of use, compact Nusselt number expressions are presented with the coefficients listed in Tables for some values of the independent variables. To obtain accurate results for other conditions, the interested reader is advised to download the fortran codes made available at the following web site: http://paginas.fe.up.pt/~fpinho/research/menur.html under "heat transfer".

Acknowledgements

The authors are grateful to the helpful comments made by the reviewers and FT Pinho acknowledges funding by FEDER and Fundação para a Ciência e a Tecnologia through grants POCI/EQU/56342/2004 and POCI/EME/59338/2004.

Appendix A

Throughout this appendix variables S_1 to S_5 are used for compactness, which are defined as $S_1=\kappa^2+1$, $S_2=\kappa^4+S_1$, $S_3=\kappa^6+S_2$, $S_4=\kappa^8+S_3$ and $S_5=\kappa^{10}+S_4$.

Coefficients of the bulk temperature Eq. (45) for imposed wall heat flux

$$A_1 = \frac{\Lambda^2\Psi(\kappa^2+1)}{2\kappa^2}; \quad A_2 = A_{21}(\ln\kappa)^2 + A_{22}\ln\kappa + A_{23}$$

$$A_{21} = \frac{\Lambda y_*^{+2}[2\varphi\Psi - \beta(4\Omega-1)]}{\kappa^2-1} \quad \text{and} \quad A_{22} = A_{21} + \frac{\Lambda\Omega\beta\kappa^2 y_*^{+4} + \Lambda(\Lambda\Psi\kappa^2 - 2c_2)}{1-\kappa^2}$$

$$A_{23} = \frac{\Lambda S_2[5\Lambda\Psi + \beta(4\Omega-1)]}{24\kappa^4 y_*^{+2}} - \frac{\Lambda S_3(10\varphi\Psi + \beta\Omega)}{72\kappa^6 y_*^{+4}} - \frac{\Lambda y_*^{+2}(4\varphi\Psi - 4\beta\Omega + \beta)}{2} + \frac{\Lambda[(3\Lambda\Psi - 6\beta\Omega + 2\Psi c_1 + 2\beta)S_1 - 4\kappa^2(c_2 - 2c_3)}{4\kappa^2}$$

$$B_1 = \frac{2\kappa^2 y_*^{+4}\varphi B_{11}}{3(\kappa^2-1)} \quad \text{with} \quad B_{11} = 2\varphi\Psi - \beta(4\Omega-1)$$

$$B_2 = \frac{\Lambda\Omega\beta\kappa^2 y_*^{+4}}{2(\kappa^2-1)} + \frac{y_*^{+2}[2\varphi(2c_2\kappa^2 + \Psi(\Lambda+c_1)) + \beta(1-4\Omega)(\Lambda+c_1)]}{2(\kappa^2-1)} + \frac{\varphi B_{11}}{6\kappa^4 y_*^{+2}(1-\kappa^2)} + \frac{\Lambda(B_{11} + 2\Lambda\Psi\kappa^4)}{4\kappa^2(\kappa^2-1)}$$

$$B_3 = \frac{\Omega\beta c_1\kappa^2 y_*^{+4} - y_*^{+2}\{2\varphi[2\Lambda\Psi S_1 + \Psi c_1 - 4c_3\kappa^2] + \beta(1-4\Omega)[\Lambda(\kappa^2+2) + c_1]\}}{2(1-\kappa^2)} + \frac{\varphi[8\varphi\Psi + 4\beta(1-4\Omega)] + 3\Lambda\kappa^2[\kappa^4(5\Lambda\Psi + 4\Omega\beta - \beta) - 12c_2]}{72\kappa^4 y_*^{+2}(1-\kappa^2)} - \frac{2\varphi(5\Lambda\Psi\kappa^6 - 12c_2) + \Lambda\Omega\beta\kappa^6}{72\kappa^4 y_*^{+4}(1-\kappa^2)} - \frac{2\Psi\Lambda(\varphi - 3\Lambda\kappa^4) + \Lambda[4\kappa^4(3\beta\Omega - \Psi c_1 - \beta + 2(c_2 - 2c_3)) + \beta(1-4\Omega) + 8\kappa^2 c_2] + 8c_1c_2\kappa^2}{8\kappa^2(1-\kappa^2)}$$

$$B_4 = \frac{\varphi\Omega\beta\kappa^2 y_*^{+6}}{2} + \frac{y_*^{+2}\{\beta[\Lambda(11\Omega-3) + c_1(4\Omega-1)] - 4\varphi[3(\Lambda\Psi - \beta\Omega) + \Psi c_1 + \beta]\}}{4} + \frac{3\{29\Lambda^2\Psi S_2 - \Lambda[(68\beta\Omega - 15\Psi c_1 - 23\beta)S_2 + 18\kappa^2(c_2 - 4c_3)S_1] + 3\beta c_1 S_2(4\Omega-1)\}}{432\kappa^4 y_*^{+2}} + \frac{4\varphi S_2[4\varphi\Psi + \beta(1-2\Omega)]}{432\kappa^4 y_*^{+2}} + \frac{S_3[9\Lambda^2\Psi + \Lambda\beta(35\Omega-9) - 4\Omega\beta c_1]}{576\kappa^6 y_*^{+4}} - \frac{2\varphi\{41\Lambda\Psi S_3 - 4[(27\Omega\beta - 5\Psi c_1 - 9\beta)S_3 + 4\kappa^2(c_2 - 6c_3)S_2]\}}{576\kappa^6 y_*^{+4}} - \frac{S_4\{\varphi[13\Lambda\Psi + 9\beta(4\Omega-1)] + 4\Lambda\Omega\beta\}}{720\kappa^8 y_*^{+6}} + \frac{\varphi S_5(\varphi\Psi + \Omega\beta)}{216\kappa^{10} y_*^{+8}} - \frac{2S_1\{\Psi[\Lambda(2\varphi - 3\Lambda - 6c_1) - 2c_1^2] + \varphi\beta(2\Omega-1)\} + \Lambda[(8\Omega-3)\beta S_1 + 32\kappa^2(c_2 - c_3)]}{32\kappa^2} - \frac{8c_1[(3\Omega-1)\beta S_1 + 2\kappa^2(c_2 - 2c_3)]}{32\kappa^2}$$

Coefficients of the bulk temperature Eq. (45) for imposed wall temperature

$$D_1 = \frac{\Lambda\beta y_*^{+2}(4\Omega-1)}{1-\kappa^2}$$

$$D_2 = \Lambda\frac{\Omega\beta\kappa^2 y_*^{+4} + \beta y_*^{+2}(4\Omega-1) - 2c_4}{1-\kappa^2}$$

$$D_3 = \Lambda\left\{(2c_5 - c_4) + \beta\left[\frac{y_*^{+2}(4\Omega-1)}{2} + \frac{S_1(1-3\Omega)}{2\kappa^2} + \frac{S_2(4\Omega-1)}{24\kappa^4 y_*^{+2}} - \frac{S_3\Omega}{72\kappa^6 y_*^{+4}}\right]\right\}$$

$$D_4 = \frac{2\varphi\beta\kappa^2 y_*^{+4}(4\Omega - 1)}{3(1-\kappa^2)}$$

$$D_5 = \frac{2\varphi c_4\kappa^2 y_*^{+2}}{\kappa^2 - 1} + \frac{\Lambda\Omega\beta\kappa^2 y_*^{+4} - \beta y_*^{+2}(\Lambda + c_1)(4\Omega - 1)}{2(\kappa^2 - 1)} - \frac{\Lambda\beta(4\Omega - 1)}{4\kappa^2(\kappa^2 - 1)} + \frac{\varphi\beta(4\Omega - 1)}{6\kappa^4 y_*^{+2}(\kappa^2 - 1)}$$

$$D_6 = \frac{c_4(\Lambda S_1 + c_1) - 2c_5\kappa^2(2\varphi y_*^{+2} + \Lambda)}{\kappa^2 - 1} - \frac{\Omega\beta c_1\kappa^2 y_*^{+4} + \beta y_*^{+2}(4\Omega - 1)[\Lambda(\kappa^2 + 2) + c_1]}{2(\kappa^2 - 1)} + \frac{c_4}{\kappa^2 - 1}\left[\frac{\Lambda}{2\kappa^2 y_*^{+2}} - \frac{\varphi}{3\kappa^4 y_*^{+4}}\right]$$
$$+ \frac{\beta(4\Omega - 1)(4\varphi - 3\Lambda\kappa^6)}{72\kappa^4 y_*^{+2}(\kappa^2 - 1)} + \frac{\Lambda\Omega\beta\kappa^2}{72 y_*^{+4}(\kappa^2 - 1)} + \frac{\Lambda\beta[4\Omega(3\kappa^4 - 1) - 4\kappa^4 + 1]}{8\kappa^2(\kappa^2 - 1)}$$

$$D_7 = c_5(\Lambda + c_1) - \frac{c_4(2\Lambda + c_1) - \varphi\Omega\beta\kappa^2 y_*^{+6}}{2} + \frac{\beta y_*^{+2}[4\varphi(3\Omega - 1) + \Lambda(11\Omega - 3) + c_1(4\Omega - 1)}{4} + \frac{\Lambda S_1(4c_5 - c_4)}{8\kappa^2 y_*^{+2}}$$
$$+ \frac{\varphi S_2(c_4 - 6c_5)}{18\kappa^4 y_*^{+4}} - \frac{\beta S_1[2\varphi(2\Omega - 1) + \Lambda(8\Omega - 3) + 8c_1(3\Omega - 1)]}{32\kappa^2}$$
$$- \frac{\beta S_2\{4\varphi(2\Omega - 1) + 3[\Lambda(68\Omega - 23) - 3c_1(4\Omega - 1)]\}}{432\kappa^4 y_*^{+2}} + \frac{\beta S_3[72\varphi(3\Omega - 1) + \Lambda(35\Omega - 9) - 4\Omega c_1]}{576\kappa^6 y_*^{+4}}$$
$$- \frac{\beta S_4[9\varphi(4\Omega - 1) + 4\Lambda\Omega]}{720\kappa^8 y_*^{+6}} + \frac{\varphi\Omega\beta S_5}{216\kappa^{10} y_*^{+8}}$$

References

[1] R.K. Shah, A.L. London, Laminar Flow Forced Convection in Ducts, Academic Press, New York, 1978.

[2] W.M. Kays, M.E. Crawford, B. Weigand, Convective Heat and Mass Transfer, fourth ed., McGraw-Hill, New York, 2004.

[3] J.-F. Agassant, P. Avenas, J.-Ph. Sergent, P.J. Carreau, Polymer Processing, Principles and Modeling, Hanser Publishers, Munich, 1991.

[4] N. Phan-Thien, R.I. Tanner, A new constitutive equation derived from network theory, J. Non-Newt. Fluid Mech. 2 (1977) 353–365.

[5] N. Phan-Thien, A nonlinear network viscoelastic model, J. Rheol. 22 (1978) 259–283.

[6] R.B. Bird, J.M. Wiest, Constitutive equations for polymeric liquids, Annual Rev. Fluid Meek 27 (1995) 169–193.

[7] H. Lamb, Hydrodynamics, sixth ed., Cambridge University Press, Cambridge, UK, 1932.

[8] A.G. Fredrikson, R.B. Bird, Non-Newtonian flow in annuli, Ind. Eng. Chem. 50 (1958) 347–352.

[9] R.W. Hanks, The axial laminar flow of yield-pseudoplastic fluids in a concentric annulus, Ind. Eng. Chem. Proces. Des. Dev. 18 (1979) 488–493.

[10] F.T. Pinho, P.J. Oliveira, Axial annular flow of a nonlinear viscoelastic fluid—an analytical solution, J. Non-Newt. Fluid Mech. 93 (2000) 325–337.

[11] D.O.A. Cruz, F.T. Pinho, Skewed Poiseuille-Couette flows of SPTT fluids in concentric annuli and channels, J. Non-Newt. Fluid Mech. 121 (2004) 1–14.

[12] M.P. Escudier, P.J. Oliveira, F.T. Pinho, Fully developed laminar flow of purely viscous non-Newtonian liquids through annuli, including the effects of eccentricity and inner-cylinder rotation, Int. J. Heat Fluid Flow 23 (2002) 52–73.

[13] Y.A. Çengel, Heat Transfer, A Practical Approach, second ed., McGraw-Hill, New York, 2003.

[14] K. Lundberg, W.C. Reynolds, W.M. Kays, Heat transfer with laminar flow in concentric annuli with constant and variable wall temperature and heat flux. Internal report AHT-2, Dept. Mech. Eng., Stanford University, Stanford, California, 1961.

[15] K. Lundberg, P.A. McCuen, W.C. Reynolds, Heat transfer in annular passages. Hydrodynamically developed laminar flow with arbitrarily prescribed wall temperatures or heat fluxes, Int. J. Heat Mass Transfer 6 (1963) 495–529.

[16] H.C. Brinkman, Heat effects in capillary flow I, Appl. Sci. Res. A 2 (1951) 120–124.

[17] J.W. Ou, K.C. Cheng, Viscous dissipation effects on thermal entrance in laminar and turbulent pipe flows with uniform wall temperature, Paper ASME 74-HT-50, AIAA/ASME 1974 Thermophysics and Heat Transfer Conference, Boston, MA, 15-17 July 1974.

[18] H.L. Toor, Heat transfer in forced convection with internal heat generation, AIChE J. 4 (3) (1958) 319–323.

[19] W.N. Gill, Heat transfer in laminar power law flows with energy sources, AIChE J. 8 (1) (1962) 137–138.

[20] G. Forrest, W.L. Wilkinson, Laminar heat transfer to power law fluids in tubes with constant wall temperature, Trans. Inst. Chem. Engrs. 51 (1973) 331–338.

[21] O. Jambal, T. Shigechi, G. Davaa, S. Momoki, Effects of viscous dissipation and fluid axial heat conduction on heat transfer for non-Newtonian fluids in ducts with uniform wall temperature. Part I: Parallel plates and circular ducts, Int. Comm. Heat Mass Transfer 32 (2005) 1165–1173.

[22] R.L. Batra, V.R. Sudarsan, Laminar flow and heat transfer in the entrance region of concentric annuli for power law fluids, Comput. Meth. Appl. Mech. Eng. 95 (1992) 1–16.

[23] M. Capobianchi, T.F. Irvine, Predictions of pressure drop and heat transfer in concentric annular ducts with modified power law fluids, Wärme u Stoffübertr. 27 (1992) 209–215.

[24] S.-N. Hong, J.C. Matthews, Heat transfer to non-Newtonian fluids in laminar flow through concentric annuli, Int. J. Heat Mass Transfer 12 (1969) 1699–1703.

[25] M. Naimi, R. Devienne, M. Lebouche, Etude dynamique et thermique de l'ecoulement de Couette- Taylor- Poiseuille; cas d'un fluide presentant un seuil d'écoulement, Int. J. Heat Mass Transfer 33 (1990) 381–391.

[26] C. Nouar, R. Devienne, M. Lebouche, Convection thermique pour l'ecoulement de Couette avec débit axial; cas d'un fluide pseudo-plastique, Int. J. Heat Mass Transfer 30 (1987) 639–647.

[27] K.K. Raju, R. Devanathan, Heat transfer to non-Newtonian fluids in laminar flow through concentric annuli with or without suction, Rheol. Acta 10 (1971) 484–492.
[28] M. Tanaka, N. Mitsuishi, Non-Newtonian laminar heat transfer in concentric annuli, Kagaku-Kogaku 38 (1974) 664–671, in Japanese.
[29] M. Tanaka, N. Mitsuishi, Non-Newtonian laminar heat transfer in concentric annuli, Heat Transfer Jpn. Res. 4 (1975) 26–36.
[30] S.H. Lin, Heat transfer to generalized non-Newtonian Couette flow in annuli with moving outer cylinder, Int. J. Heat Mass Transfer 35 (11) (1992) 3069–3075.
[31] O. Jambal, T. Shigechi, G. Davaa, S. Momoki, Effects of viscous dissipation and fluid axial heat conduction on heat transfer for non-Newtonian fluids in ducts with uniform wall temperature. Part II: Annular ducts, Int. Comm. Heat Mass Transfer 32 (2005) 1174–1183.
[32] P.M. Coelho, F.T. Pinho, Fully-developed heat transfer in annuli with viscous dissipation, Int. J. Heat Mass Transfer, 2006, in press.
[33] R.M. Manglik, P. Fang, Effect of eccentricity and thermal boundary conditions on laminar flow in annular ducts, Int. J. Heat Fluid Flow 16 (1995) 298–306.
[34] P. Fang, R.M. Manglik, M.A. Jog, Characteristics of laminar viscous shear-thinning fluid flows in eccentric annular channels, J. Non-Newt. Fluid Mech. 84 (1999) 1–17.
[35] P. Fang, R.M. Manglik, Numerical investigation of laminar forced convection in Newtonian and non-Newtonian flows in eccentric annuli, Technical report TFTPL-3, Dept. Mechanical, industrial and Nuclear Engineering, University of Cincinnati, USA, 1998.
[36] A.I. Leonov, Nonequilibrium thermodynamics and rheology of viscoelastic polymer media, Rheol. Acta 15 (2) (1976) 85–98.
[37] A.I. Leonov, On a class of constitutive equations for viscoelastic liquids, J. Non-Newt. Fluid Mech. 25 (1987) 1–59.
[38] P. Wapperom, M.A. Hulsen, Thermodynamics of viscoelastic fluids: the temperature equation, J. Rheol. 42 (5) (1998) 999–1019.
[39] G.W.M. Peters, F.P.T. Baaijens, Modelling of non-isothermal viscoelastic flows, J. Non-Newt. Fluid Mech. 68 (1997) 205–224.
[40] P. Wapperom, Non-isothermal flows of viscoelastic fluids, Thermodynamics, analysis and numerical simulation, PhD thesis, Delft University of Technology, Holland, 1995.
[41] G. Astarita, G.C. Sarti, The dissipative mechanism in flowing polymers, J. Non-Newt. Fluid Meek 1 (1976) 39–50.
[42] T. Nikoleris, R. Darby, Numerical simulation of the non-isothermal flow of a nonlinear viscoelastic fluid in a rectangular channel, J. Non-Newt. Fluid Meck 31 (1989) 193–207.
[43] R.I. Tanner, Engineering Rheology, first ed., Clarendon Press, 1985.
[44] G.C. Sarti, N. Esposito, Testing thermodynamic constitutive equations for polymers by adiabatic deformation experiments, J. Non-Newt. Fluid Meek 3 (1977/1978) 65–76.
[45] P.J. Oliveira, F.T. Pinho, Analysis of forced convection in pipes and channels with the simplified Phan-Thien–Tanner fluid, Int. J. Heat Mass Transfer 43 (13) (2000) 2273–2287.